NASA Goddard Space Flight Center's Current Radiation Effects Test Results

Martha V. O'Bryan, Edward P. Wilcox, Thomas A. Carstens, Kaitlyn L. Ryder, Jonathan D. Barth, Jason M. Osheroff, Landen D. Ryder, Megan C. Casey, Matthew B. Joplin, Jean-Marie Lauenstein, Kenneth A. LaBel, Michael J. Campola, Edward J. Wyrwas, Aubin P. Antonsanti, Melanie D. Berg, Donna J. Cochran, Peter J. Majewicz, and Jonathan A. Pellish

Abstract-- We present results and analysis investigating the effects of radiation on a variety of candidate spacecraft electronics to heavy ion and proton induced single event effects (SEE), proton-induced displacement damage dose (DDD), and total ionizing dose (TID).

I. INTRODUCTION

NASA spacecraft are subjected to a harsh space environment that includes exposure to various types of radiation. The performance of electronic devices in a space radiation environment is often limited by its susceptibility to single-event effects (SEE), total ionizing dose (TID), and displacement damage dose (DDD). Ground-based testing is used to evaluate candidate spacecraft electronics to determine risk to spaceflight applications. Interpreting the results of radiation testing of complex devices is quite difficult. Given the rapidly changing nature of technology, radiation test data are most often application-specific and adequate understanding of the test conditions is critical [1].

Studies discussed herein were undertaken to establish the application-specific sensitivities of candidate spacecraft and emerging electronic devices to single-event SEE including single-event upset (SEU), single-event latchup (SEL), single-event gate rupture (SEGR), single-event burnout (SEB), single-event transient (SET), TID, enhanced low dose rate sensitivity (ELDRS), and DDD effects. All tests were performed between February 2022 and February 2023.

II. TEST TECHNIQUES AND SETUP

A. Test Method

Unless otherwise noted, SEE testing was performed in accordance with JESD57A test procedures [2]. Depending on the Device Under Test (DUT) and the test objectives, one or two SEE test methods were typically used:

a) *Dynamic* – The DUT was exercised and monitored continuously while being irradiated. The type of input stimulus and output data capture methods are highly device- and application-dependent. In all cases the power supply levels were actively monitored during irradiation. These results are highly application-dependent and may only represent the specific operational mode tested.

b) *Static/Biased* – The DUT was provided basic power and configuration information (where applicable), but not actively operated during irradiation. The device output may or may not have been actively monitored during irradiation, while the power supply current was actively monitored for changes.

In SEE experiments, DUTs were monitored for soft errors, such as SEUs, and for hard errors, such as SELs. Detailed descriptions of the types of errors observed are noted in the individual test reports.

SET testing was performed using high-speed oscilloscopes controlled via National Instruments LabVIEW® [3]. Individual criteria for SETs are specific to the device and application being tested. Please see the individual test reports for details [4. 5].

Heavy ion SEE sensitivity experiments include measurement of the linear energy transfer threshold (LET_{th}) and cross section at the maximum measured LET. The LET_{th} is defined as the maximum LET value at which no effect was observed at an effective fluence of 1×10^7 particles/cm^2. In the case where events are observed at the smallest LET tested, LET_{th} will either be reported as less than the lowest measured LET or determined approximately as the LET_{th} parameter from a Weibull fit.

TID testing was performed using MIL-STD-883, Test Method 1019.9 [6] unless otherwise noted as research. All tests were performed at room temperature and with nominal power supply voltages, unless otherwise noted. Based on the application, samples would be tested in a biased and/or unbiased configuration. Functionality and parametric changes were measured after step irradiations (for example: every 10 krad(Si)).

B. Test Facilities – SEE

Heavy ion experiments were conducted at the Texas A&M University Cyclotron (TAMU) [7], Lawrence Berkeley National Laboratory (LBNL) 88-inch cyclotron [8], and Brookhaven National Laboratory's NASA Space Radiation Laboratory (NSRL) [9]. These facilities provide a variety of ions over a range of energies for testing.

This work was supported in part by the NASA Electronic Part and Packaging Program (NEPP) and NASA Flight Projects.

Martha V. O'Bryan, Kenneth A. LaBel, Edward J. Wyrwas, Melanie Berg, and Donna J. Cochran, are with SSAI, work performed for NASA Goddard Space Flight Center, Code 561.4, Greenbelt, MD 20771 (USA), phone: 301-286-1412, email: martha.v.obryan@nasa.gov.

Edward P. Wilcox, Thomas A. Carstens, Kaitlyn L. Ryder, Jonathan D. Barth, Jason M. Osheroff, Landen D. Ryder, Megan C. Casey, Matthew B. Joplin, Jean-Marie Lauenstein, Michael J. Campola, Aubin P. Antonsanti, Jonathan A. Pellish, and Peter J. Majewicz are with NASA/GSFC, Code 561.4, Greenbelt, MD 20771 (USA), phone: 301-286-5427, email: ted.wilcox@nasa.gov.

C. Test Facilities – TID

TID testing was performed using a gamma source [10]. Dose rates used for testing were between 10 mrad(Si)/s and 2.6 krad(Si)/s.

D. Test Facilities – DDD

Proton DDD tests were performed at the University of California at Davis Crocker Nuclear Laboratory (UCD - CNL) [11] using a 76" cyclotron and energy of 64 MeV.

III. TEST RESULTS OVERVIEW

Principal investigators are listed in Table I. Abbreviations and conventions are listed in Table II. SEE results are summarized in Table III. TID and DDD results are summarized in Table IV. All parts tested between March 2022 and February 2023. Unless otherwise noted all LETs are in MeV•cm^2/mg and all cross sections are in cm^2/device. All SEL tests are performed to a fluence of 1×10^7 particles/cm^2 unless otherwise noted. Proton tests were performed at a flux of $1x10^7$ to $1x10^9$ p$^+$/cm^2-s. The fluence was to until an event was observed, or $1x10^{10}$ to $1x10^{11}$ p$^+$/cm^2 at a given energy (i.e. 200 MeV, etc).

TABLE I: LIST OF PRINCIPAL INVESTIGATORS

Principal Investigator (PI)	Abbreviation
Aubin Antonsanti	AA
Jonathan D. Barth	JB
Melanie D. Berg	MB
Michael J. Campola	MJC
Thomas A. Carstens	TAC
Megan C. Casey	MCC
Matthew B. Joplin	MBJ
Kaitlyn L. Ryder	KLR
Jason M. Osheroff	JMO
Landen D. Ryder	LR
Edward (Ted) Wilcox	TW
Edward J. Wyrwas	EW

TABLE II: ACRONYM LIST

Acronym	Definition
σ	cross section (cm^2/device, unless specified as cm^2/bit)
σ_{maxm}	cross section at maximum measured LET (cm^2/device, unless specified as cm^2/bit)
<	SEE observed at lowest tested LET
>	no SEE observed at highest tested LET
BiCMOS	Bipolar-Complementary Metal Oxide Semiconductor
Block SEFI	Interruption in access to one or more memory blocks
CMOS	Complementary Metal Oxide Semiconductor
DC	Dark Current
DDD	Displacement Damage Dose
DUT	Device Under Test
FPGA	Field Programmable Gate Array
GPU	Graphic Processing Unit
GSFC	Goddard Space Flight Center
LBNL	Lawrence Berkeley National Laboratory
LDC	Lot Date Code
LET	Linear Energy Transfer
LET_{th}	Linear Energy Transfer threshold (the maximum LET value at which no effect was observed at an effective fluence of $1x10^7$ particles/cm^2 – in MeV•cm^2/mg
MEMS	Micro Electro Mechanical Systems
MOSFET	Metal-Oxide-Semiconductor Field-Effect Transistor
NEPP	NASA Electronics Parts and Packaging
OLED	Organic Light Emitting Diode
Op Amp	Operational Amplifier
PI	Principal Investigator
REAG	Radiation Effects & Analysis Group
SEE	Single-Event Effect
SEFI	Single-Event Functional Interrupt
SEL	Single-Event Latchup
SET	Single-Event Transient
SEU	Single-Event Upset
SLC	Single-Level Cell
TAMU	Texas A&M University
TFT	Thin Film Transistor
TLC	Triple-Level Cell
TID	Total Ionizing Dose
UCD-CNL	University of California at Davis Crocker Nuclear Laboratory
V_{DS}	Drain-Source Voltage
V_{GS}	Gate-Source Voltage

TABLE III: SUMMARY OF SEE TEST RESULTS

Part Number	Manufacturer	LDC (REAG ID#)	Device Function	Technology	PI	Sample Size	Supply Voltage	Test Env.	Test Facility (Test Date)	Test Results: σ in cm²/device, unless otherwise specified
Processors & FPGAs										
Radeon e9173	AMD	n/a; (19-022)	GPU	CMOS	EW	3	12 V	Heavy Ion	LBNL (Aug 2022)	SEL LET_{th} > 16 MeV•cm²/mg; Unstable electrical behavior observed above 60°C showing reduced framerate and computational speed. [12]
Neural Compute Stick 2	Intel	n/a; (22-002)	Vision Processing Unit	Si	MCC	1	3.3 V and 1.8 V	Heavy Ion	LBNL (Apr 2022)	SEL LET_{th} > 49.3 MeV•cm²/mg; SEFI LET_{th} < 1.16 MeV•cm²/mg. [13]
								Protons	MGH (May 2022)	Recoverable and nonrecoverable SEFIs observed with 60, 125, and 200 MeV protons. [13]
Coral Accelerator Module	Google	n/a; (22-001)	Tensor Processing Unit	Si	MCC	2	5 V	Heavy Ion	NSRL (Mar 2022)	SEL LET_{th} > 57.3 MeV•cm²/mg; 0.5 MeV•cm²/mg < SEFI LET_{th} < 1.96 MeV•cm²/mg 43.04 MeV•cm²/mg < Stuck bits LET_{th} < 57.3 MeV•cm²/mg. [13]
AMD v1202b	AMD	n/a (20-005)	CPU	CMOS	EW	1	12 V	Protons	MGH (May 2022)	SEFIs were observed, but all were recoverable. Average SEFI σ was $3.58x10^{-10}$ cm² at 200 MeV. [14]
A3PE3000-1PQG208I	Microchip/ Actel	1108 (n/a)	ProASIC FPGA	CMOS	MB	3	1.5V; 1.8V; and 3.3V	Heavy Ion	LBNL (Apr 2022) and TAMU (Jun 2022)	Application specific SEE characterization. Contact PI [15]
Memories										
MT29F16G08ABABA	Micron	2204; (22-009)	Flash Memory	NAND	TW	4	3.3 V	Heavy Ion	LBNL (Apr 2022)	Block SEFI LET_{th} < 2.64 MeV•cm²/mg; Block SEFI σ_{maxm} ~$4x10^{-8}$ cm²/block (LET=25 MeV•cm²/); Further detailed results available [16] [17] (contact PI)
H25G9TC18CX488	SKHynix	212T; (22-044)	Flash Memory	3D NAND	TW	1	3.3 V	Heavy Ion	LBNL (Nov 2022)	56 < SEL LET_{th} < 79 MeV•cm²/mg (no destructive failures were observed); SEU LET_{th} < 3 MeV•cm²/mg; SEU σ_{maxm} (SLC) $2.63x\ 10^{-11}$ cm²/bit (LET=56 MeV•cm²/mg); SEU σ_{maxm} (TLC) $7.56x10^{-11}$ cm²/bit (LET=56 MeV•cm²/mg); SEFI LET_{th} < 8 MeV•cm²/mg [18] [19]
						2		Proton	MGH (Dec 2022)	200 MeV SEU σ (SLC) $4.31x10^{-17}$ cm²/bit 125 MeV SEU σ (SLC) $8.40x10^{-17}$ cm²/bit [20]
MT29F8T08EWLGEM5	Micron	1YG22; (22-042)	Flash Memory	3D NAND	TW	2	2.5 - 3.3 V	Heavy Ion	LBNL (Aug & Nov 2022)	SEL LEt_{th}> 79 MeV•cm²/mg at 85°C; SEU LET_{th} < 1.2 MeV•cm²/mg; SEU σ_{maxm} (SLC) $3.3x10^{-11}$ cm²/bit (LET=56 MeV•cm²/mg); SEU σ_{maxm} (TLC) $1.1x10^{-10}$ cm²/bit (LET=56 MeV•cm²/mg) [19] [21]
						1		Proton	MGH (Dec 2022)	200 MeV SEU σ (SLC) $4.13x10^{-18}$ cm²/bit 125 MeV SEU σ (SLC) $2.95x10^{-18}$ cm²/bit [20]

Part Number	Manufacturer	LDC (REAG ID#)	Device Function	Technology	PI	Sample Size	Supply Voltage	Test Env.	Test Facility (Test Date)	Test Results: σ in cm²/device, unless otherwise specified
Memories (Cont.)										
MT29F8T08EWLKEM5-ITF:K (B47T)	Micron	2PK22; (22-043)	Flash Memory	3D NAND	TW	3	2.5 - 3.3 V	Heavy Ion	LBNL (Nov 2022)	SEL LET_{th}> 79 MeV•cm²/mg at 85°C; SEU LET_{th} < 3; SEU σ_{maxm} (SLC and TLC) ~$5x10^{-11}$cm²/bit (LET=29 MeV•cm²/mg); SEFI LET_{th} < 3.0 MeV•cm²/mg [19] [22]
						1		Proton	MGH (Dec 2022)	200 MeV SEU σ (SLC) $1.41x10^{-17}$ cm²/bit [20]
4N1G72T-24BM	Mercury Systems	n/a; (n/a)	SDRAM	DDR4	MB	3	2.5 V, 1.2 V, and 0.6 V	Proton	MGH (Dec 2022)	Stuck bits were observed with 60 MeV and 200 MeV protons. Small increases in supply current (~50 mA) were also observed that may be related to the stuck bits. [23]
Power Devices										
JANSR2N7593	Microchip	C2052; (21-020)	MOSFET	Si	JMO	4	-5, -10, -15 V_{GS}	Heavy Ion	NSRL (Mar 2022)	LET =60 MeV•cm²/mg with 36.8 MeV/u Bi: no SEB/GR at 250 V_{DS} & -5 V_{GS}; 3(1) pass/(fail) at 250 V_{DS} & -10 V_{GS}. SEGR at -15 V_{GS} for 75V < V_{DS} <100V [24]
IRF5NJ9540	Infineon	n/a (22-016)	p-Type Power MOSFET	Si	JMO	4	0 V_{GS}	Heavy Ion	TAMU (Sept. 2022)	SEGR threshold -45V< V_{DS}< -50V at LET = 45 MeV•cm²/mg with 15 MeV/n Ag [25]
TC1016	Microchip	n/a; (n/a)	Low Dropout Voltage Regulator	CMOS	KLR	1	3.3 V	Heavy Ion	LBNL (Jun 2022)	SET LET_{th} = 8.2 MeV•cm²/mg σ_{maxm} = $1.1x10^{-4}$ cm² (LET = 54.5 MeV•cm²/mg); SETs with amplitudes > 2 V were examined. Durations of SETs were not recorded. SEL LET_{th} > 54.5 MeV•cm²/mg [26]
Displays										
SSD1351	Solomon Systech	n/a; (22-045)	OLED Electronic Display Segment/Common Driver IC	CMOS	LR	2	5 V	Heavy Ion	LBNL (Aug 2022)	Errors observed starting with a surface LET of 1.2 MeV•cm²/mg). Driver IC was connected to to a small OLED display for visual monitoring of SEE signatures. Error signatures were catalogued and mapped to likely location within the configuration memory of component. [27]
Analog/Linear Devices										
AD8041ARZ	Analog Devices, Inc.	2112; (22-040)	Op Amp	Bipolar	MBJ	3	±5 V	Heavy Ion	LBNL (Nov 2022)	SEL LET_{th} > 49.5 MeV•cm²/mg; SET LET_{th} < 8.5 MeV•cm²/mg;. SET σ_{maxm} = $5x10^{-5}$ cm^{-2}/mg (LET=49.5 MeV•cm²/mg) [28] Sample speed was set to 100 MS/s. SET analysis not needed by the project. Low Likelihood drove risk acceptance.
LTC3769HUF#PBF	Linear Technology	n/a; (n/a)	Boost Converter Controller	Unknown	KLR	1	12 V	Heavy Ion	LNBL (Jun 2022)	SEU LET_{th} = 8.2 MeV•cm²/mg $\sigma_{maxm,SEU}$ = $4.0x10^{-6}$ cm² (LET = 29.8 MeV•cm²/mg); SEFI LET_{th} = 8.2 MeV•cm²/mg $\sigma_{maxm,SEFI}$ = $7.4x10^{-6}$ cm² (LET = 84.3 MeV•cm²/mg); SEL LET_{th} > 84.3 MeV•cm²/mg [29]

Part Number	Manufacturer	LDC (REAG ID#)	Device Function	Technology	PI	Sample Size	Supply Voltage	Test Env.	Test Facility (Test Date)	Test Results: σ in cm²/device, unless otherwise specified
Analog/Linear Devices (Cont)										
OPA691	Texas Instruments	n/a; (n/a)	Current Feedback Op Amp	Complementary Bipolar	KLR, JB	3	V_s = ±5 V V_{in} = 2.5 V	Heavy Ion	LBNL (Nov 2022)	SET LET_{th} < 69.9 MeV•cm²/mg σ_{maxm} ~10^{-4} cm² (LET = 69.9 MeV•cm²/mg); Maximum observed SET amplitudes were Vout±1.25 V. Maximum observed SET durations were < 0.2 µs. SEL LET_{th} > 69.9 MeV•cm²/mg [30]
OPA842	Texas Instruments	n/a; (n/a)	Low-Noise Op Amp	CMOS	KLR, JB	3	V_s = ±5 V V_{in} = 1.25 V	Heavy Ion	LBNL (Nov 2022)	SET LET_{th} < 69.9 MeV•cm²/mg σ_{maxm} ~$5.2x10^{-5}$ cm² (LET = 69.9 MeV•cm²/mg) Maximum observed SET amplitudes were Vout±1.75 V. Maximum observed SET durations were < 0.1 µs. SEL LET_{th} > 69.9 MeV•cm²/mg [31]
OPA847	Texas Instruments	n/a; (n/a)	Ultra-Low Noise Op Amp	Complementary Bipolar	KLR, JB	3	V_s = ±5 V V_{in} = -50 mV, 0 V, +50 mV	Heavy Ion	LBNL (Nov 2022)	SET LET_{th} < 69.9 MeV•cm²/mg σ_{maxm} ~10^{-4} cm² (LET = 69.9 MeV•cm²/mg); Maximum observed SET amplitudes were Vout±2.5 V. Maximum observed SET durations were < 0.15 µs. SEL LET_{th} > 69.9 MeV•cm²/mg [32]
OPA855	Texas Instruments	n/a; (n/a)	Low-Noise Op Amp	BiCMOS	KLR, JB	3	V_s = ±2.5 V V_{in} = 0 V, floating	Heavy Ion	LBNL (Nov 2022)	SET LET_{th} < 66.9 MeV•cm²/mg σ_{maxm} ~10^{-5} cm² (LET = 66.9 MeV•cm²/mg); Maximum observed SET amplitudes were Vout±1.5 V. Maximum observed SET durations were < 0.2 µs. SEL LET_{th} > 104 MeV•cm²/mg [33]
OPA856	Texas Instruments	n/a; (n/a)	Low-Noise Op Amp	BiCMOS	KLR, JB	3	V_s = ±2.5 V V_{in} = -1.25 V, 0 V, +1.25 V	Heavy Ion	LBNL (Nov 2022)	SET LET_{th} < 69.9 MeV•cm²/mg σ_{maxm} ~10^{-5} cm² (LET = 69.9 MeV•cm²/mg); Maximum observed SET amplitudes were Vout±1.7 V. Maximum observed SET durations were < 0.1 µs. SEL LET_{th} > 69.9 MeV•cm²/mg [34]
RF Devices										
NBB-400	Qorvo	2045; (21-036)	MMIC Amplifier	GaAs	TAC	3	5V	Heavy Ion	LBNL (Apr 2022)	SET LET_{th} < 31 MeV•cm²/mg Some transients had amplitudes larger than 1V or less than -1V. [35]
GRF2073	Guerrilla RF	n/a; (n/a)	RF Ultra-Low Noise Amplifier	GaAs pHEMT	KLR	2	5 V	Heavy Ion	LBNL (Jun 2022)	SET LET_{th} = 57.2 MeV•cm²/mg σ_{maxm} = $1.4x10^{-7}$ cm² (LET = 57.2 MeV•cm²/mg); SEL LET_{th} > 57.2 MeV•cm²/mg [36]
GRF5110	Guerrilla RF	n/a; (n/a)	Power Low Noise Amplifier	GaAs pHEMT	KLR	2	5 V	Heavy Ion	LBNL (Jun 2022)	SET LET_{th} > 55.3 MeV•cm²/mg SEL LET_{th} > 55.3 MeV•cm²/mg [37]

Part Number	Manufacturer	LDC (REAG ID#)	Device Function	Technology	PI	Sample Size	Supply Voltage	Test Env.	Test Facility (Test Date)	Test Results: σ in cm²/device, unless otherwise specified
Miscellaneous										
HVS-VAC03k, HVS-VAC04	Heimann Sensor GmbH	n/a; (22-011)	MEMS Pirani Pressure Sensor	MEMS	MCC	2	2.1V (03k); 1.2V (04)	Heavy Ion	NSRL (Mar 2022)	SEL LET_{th} > 49.3 MeV•cm²/mg [38]
									LBNL (Feb 2022)	SEL LET_{th} > 39.2 MeV•cm²/mg [38]
LMX24485ESQ/NOPM	Texas Instruments	n/a; (n/a)	Phase Locked Loop	BiCMOS	KLR	1	3 V	Heavy Ion	LBNL (Jun 2022)	SEU LET_{th} < 8.2 MeV•cm²/mg $\sigma_{maxm,SEU}$ = 4.9x10^{-5} cm² (LET = 82.9 MeV•cm²/mg) SEFI LET_{th} = 19.5 MeV•cm²/mg $\sigma_{maxm,SEFI}$ = 2.5x10^{-5} cm² (LET = 82.9 MeV•cm²/mg) SEL LET_{th} = 12.4 MeV•cm²/mg $\sigma_{maxm,SEL}$ = 3.5x10^{-5} cm² (LET = 82.9 MeV•cm²/mg) [39]
DRV8881	Texas Instruments	n/a; (22-014)	2.5A Dual H-Bridge Motor Driver	Bipolar/ MOSFET	TAC	10	24 V	Heavy Ion	LBNL (Nov 2022)	SEFI LET_{th} < 8 MeV•cm²/mg Multiple SEFI signatures No destructive events [40]
MAX1340	Maxim	n/a; (22-015)	12-Bit, Multi-channel ADC/DAC	BiCMOS	TAC	2	Digital: 3.3 V Analog: 5 V	Heavy Ion	LBNL (Nov 2022)	SEL LET_{th} > 8 MeV•cm²/mg with 16 MeV/n Ar [41]
TLE4309	Infineon	n/a; (22-013)	Adjustable Linear Low Dropout LED Driver	Bipolar	TAC	10	24 V	Heavy Ion	LBNL (Nov 2022)	SET LET_{th} < 51.7 MeV•cm²/mg [42]
ACPL-785E	Broadcom	1649, (17-047)	Analog Isolation Amplifier	CMOS	MJC	3	5 V	Heavy Ion	NSRL (Mar 2022)	4x increase in supply current [43] [44]

TABLE VI: SUMMARY OF TID and DDD TEST RESULTS

Part Number	Manufacturer	LDC or Wafer#, (REAG ID#)	Device Function	Technology	PI	Sample Size	Test Env.	Test Facility (Test Date)	Test Results (Effect, Dose Level/Energy, Results)
Processors & FPGAs									
LIFCL-40-8BG40	Lattice Semiconductor	2048; (21-016)	FPGA	Programmable Device	MB	5	Gamma	GSFC (Aug 2022)	Five (5) FPGA embedded design/components were tested: Shift register, PLL, DSP, SERDES, and ADC. Each design/component was tested in four (4) devices. All samples passed at 200 krad(Si). First failure on one sample observed after next irradiation step at 250 krad(Si). The mechanism of failure seemed to be JTAG related. Further investigation is required. [45]
Power Device									
PE99155	Teledyne	16480, 17213, 17245, 112572 (19-001)	Point-Of-Load Buck Regulator	UltraCMOS	TAC	10	Gamma	GSFC (Feb 2022)	Application specific dose testing on startup behavior. Contact PI [46]
Isolation Devices									
53253	Micropac	2138 (22-039)	Solid State Relay	Hybrid Optocoupler	TW	8	Protons	UCD (May 2022)	Functional > 97.7 krad (Si); Parametric failures > 50 krad (Si) [47]
53111	Micropac	1934; (21-030)	Solid State Relay	Hybrid	TW	6	Protons	UCD (May 2022)	Functional > 100 krad(Si); Off-state leakage current > 1mA, > 50 krad(Si) [48]
66212	Micron	2122; (22-054)	Optocoupler	Hybrid	TW	20	Protons	UCD (May 2022)	Functional > 97.7 krad (Si); Parametric failures > 11 krad (Si) [49]
Displays									
2478	Adafruit	n/a; (22-046)	Liquid Crystal Display - TFT	Optoelectronic	LR	5	Protons	UCD (Sept 2022)	<10% degradation in luminous intensity of the display with a white screen at 100 krad (Si). Minor amount of radiation-induced color shift was observed. [50] [51]
1431	Adafruit	n/a; (22-045)	OLED Display - Passive Matrix	Optoelectronic	LR	4	Protons	UCD (Sept 2022)	<15% degradation in luminous intensity of the display with a white screen at 100 krad (Si). Minor amount of radiation-induced color shift was observed. [50] [51]
KWM-20882XWB	Luckylight	n/a; (22-048)	LED Matrix - White	Optoelectronic	LR	3	Protons	UCD (Sept 2022)	<15% degradation in luminous intensity at 100 krad (Si). No radiation-induced color shift was observed. [50] [51]
4868	Adafruit	n/a; (22-051)	Electronic Ink/Paper Display - Tricolor	Optoelectronic	LR	2	Protons	UCD (Sept 2022)	No observable perturbation of a static image up to a dose of 100 krad (Si). [50] [51]
Miscellaneous									
HVS-VAC03k, HVS-VAC04	Heimann Sensor GmbH	n/a (22-011)	MEMS Pirani pressure sensor	MEMS	MCC	2	Protons	UCD (May 2022)	No degradation observed up to $3.3x10^{11}$ 63 MeV protons (45 krad(Si)). [52]
IMX219PQ	Sony	n/a; (22-052)	Image Sensor	CMOS	AA	10	Gamma	GSFC (Nov 2022)	No degradation observed up to 250 krad(Si) on biased and sequenced parts. Dark Current (DC) increase and DC Random Telegraph Signal noise occurs over 250 krad(Si). No failure up to 2 Mrad(Si). [53]
C30665L CD3740	Excelitas	05/21/20 (21-029)	Photodiode	InGaAs	LR	4	Protons	UCD (May 2022)	Optical photodiode linearity measurements showed ~20% decrease in responsivity by $7.54x10^{11}$ 63 MeV protons (100 krad(Si)). [54]

IV. TEST RESULTS AND DISCUSSION

As in our past workshop compendia of GSFC test results, most devices under test have a detailed test report available online at http://radhome.gsfc.nasa.gov [4] and at http://nepp.nasa.gov [5] describing in further detail the test method, conditions, monitored parameters, and test results. This section contains a summary of testing performed on a selection of featured parts. Due to page limitations, this section contains only one featured part; however, the final data workshop submission will contain several summaries of testing performed on a selection of featured parts.

A. Hynix H25G9TC18CX488 3D NAND Flash Memory

The H25G9TC18CX488 is a 512 Gb NAND flash manufactured by SK Hynix in their V7 3D NAND process, a 176 layer, triple-level cell (TLC), charge trap-based memory technology. The device tested is a single-die variant totaling 512 Gb; higher total capacities are also available by combining multiple die into a single plastic BGA package.

To evaluate this 176-layer process for possible use in spaceflight, and to compare trends with previous high-density non-volatile memories, the NASA Electronics Parts and Packaging (NEPP) program performed heavy-ion and 200 MeV proton single-event effects (SEE) testing at the Lawrence Berkeley National Laboratory and Massachusetts General Hospital, respectively, in the Fall of 2022.

1. Single Event Upsets

Single-event upset cross-section data from heavy-ion testing at LBNL is presented in Fig. 1, below. Each data point is a single cyclotron run at ambient temperature, with 10 blocks (~225 MB) tested in SLC and 10 blocks (~675 MB) tested in TLC. SEU testing was performed with a pseudorandom data pattern, and irradiations were performed with the device powered off to isolate memory cell errors from peripheral circuitry effects.

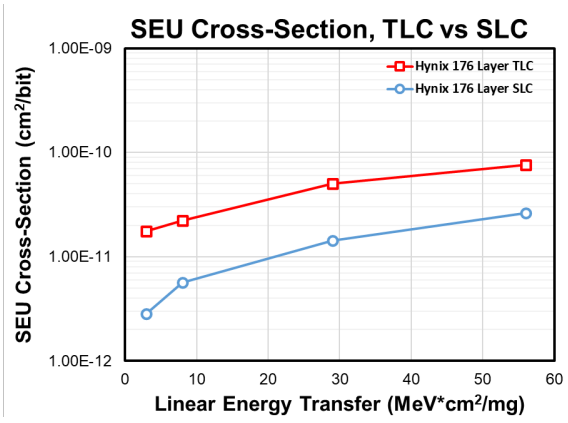

Fig. 1. Single-event upset cross-section comparison in TLC and SLC operational modes.

2. Single Event Latchup

Two tests evaluated the H25G9TC18CX488 for single-event latchup (SEL) with a 16 MeV/amu Xe beam having a surface incident LET of approximately 56 MeVcm^2/mg, with V_{CC} set to 3.3 V and the device heated to 85°C. The first, conducted at normal incidence to the device surface (effective LET ~56) found no evidence of SEL after a fluence of 1.0x10^{7}cm^{-2}. The device was not actively reading, programming, or erasing but was repeatedly queried for the device's internal ID to evaluate functionality and the power supply current monitored for signs of latchup.

The second SEL run was conducted with the device oriented at a 45 degree angle to the incoming beam (effective LET ~79) to a total fluence of 1.05x10^{7}cm^{-2}. The device did not experience any catastrophic SEL, but one event was observed that tripped the power supply's compliance limit, set to 200 mA. This event may be a single-event latchup.

3. Single Event Functional Interrupts

SEFI testing took two forms; one type of SEFI testing rapidly polled the internal ID (flash READID command) to verify basic functionality of and communications with the device while in beam. Here, any observed event was recorded and autonomously recovered using either a RESET, HARD RESET, or POWER CYCLE. The cross-section of these events that entirely disrupted operation of the memory was quite low – only a single event was observed, and it was recoverable by a HARD RESET command without subsequent power cycle.

TABLE VII: INTERNAL ID (FLASH READID COMMAND) SEFI TESTING.

LET MeVcm^2/mg	Fluence/cm^2	Count of READID SEFI resettable by		
		RESET	HARD RESET	Power Cycle
8.0	1.15 x 10^6	0	0	0
29.0	1.0 x 10^6	0	1	0

The second type of SEFI testing evaluate the susceptibility of memory blocks within the array to SEFI while irradiated during READ, PROGRAM, or ERASE operations. A total of 100 blocks were actively operated during each test. In each case, a secondary high-speed shutter was used to isolate the state of the device during active irradiation (e.g. shutter only open briefly to allow for erasing, then closed for subsequent programming and readback). The shutter was immediately closed upon detection of a SEFI event, and a power cycle was automatically employed after each ERASE-PROGRAM-READ cycle in which a SEFI was detected.

TABLE VIII: DYNAMIC ERASE, PROGRAM AND READ SEFI TESTING.

LET MeVcm^2/mg	Fluence/cm^2	Operational State While Irradiating	Count of block SEFI detected as a failure to:		
			ERASE	PROGRAM	READ
8.0	2.23 x 10^5	ERASE	390	1	385
8.0	6.58 x 10^5	PROGRAM	39	1	81
8.0	2.74 x 10^5	READ	25	0	35
29.0	1.05 x 10^5	ERASE	49	3	38
29.0	1.21 x 10^5	PROGRAM	167	66	331
29.0	6.58 x 10^5	READ	200	113	144

Note that numbers of block SEFI may be due to multiple blocks affected by a single event, and implementation and testing of any SEFI mitigation system is inherently complex and highly application specific.

V. SUMMARY

We have presented data from recent radiation tests on a variety of devices including several commercial parts. It is the authors' recommendation that this data be used cautiously as many tests were conducted under application- or lot-specific test conditions. We also highly recommend that lot-specific testing be performed on any suspect or commercial device.

VI. ACKNOWLEDGMENT

The authors would like to acknowledge the sponsors of this effort: NASA Electronic Parts and Packaging Program (NEPP) and NASA Flight Projects. The authors thank members of the Radiation Effects and Analysis Group (REAG) who contributed to the test results presented here; Alyson Topper (now with Code 565), Rebekah Austin, Stephen K. Brown, Martin A. Carts, Stephen R. Cox, Yevgeniy Gerashchenko, James Forney, Hak Kim, Kenneth LaBel, Ray Ladbury, Kenny O'Connor, Anthony Phan, Kaitlyn Ryder, Scott Stansberry, Scott Linton, Craig Stauffer, Carl Szabo, Mike Xapsos, Kevin Lynaugh and Gianfranco Barnaba from Vulcan Wireless, Serhat Altunc from NASA GSFC, Code 566, and Richard Hare from NASA LaRC, D211.

VII. REFERENCES

1. Kenneth A. LaBel, Lewis M. Cohn, and Ray Ladbury, "Are Current SEE Test Procedures Adequate for Modern Devices and Electronics Technologies?," http://radhome.gsfc. nasa.gov/ radhome/papers/HEART08_LaBel.pdf.
2. JEDEC Government Liaison Committee, Test Procedure for the Management of Single-Event Effects in Semiconductor Devices from Heavy Ion Irradiation," JESD57A, https://www.jedec.org/standards-documents/docs/jesd-57, Nov. 2017.
3. NI LabVIEW System Design Software, http://www.ni.com/labview/
4. NASA/GSFC Radiation Effects and Analysis home page, http://radhome.gsfc.nasa.gov.
5. NASA Electronic Parts and Packaging Program home page, http://nepp.nasa.gov.
6. Department of Defense "Test Method Standard Microcircuits," MIL-STD-883 Test Method 1019.9 Ionizing radiation (total dose) test procedure, June 7, 2013, https://landandmaritimeapps.dla.mil/Downloads/MilSpec/Docs/MIL-STD-883/std883.pdf.
7. B. Hyman, "Texas A&M University Cyclotron Institute, K500 Superconducting Cyclotron Facility," http://cyclotron.tamu.edu/ facilities.htm, Jul. 2003.
8. Michael B. Johnson, Berkeley Lawrence Berkeley National Laboratory (LBNL), 88-Inch Cyclotron Accelerator, Accelerator Space Effects (BASE) Facility http://cyclotron.lbl.gov.
9. Brookhaven National Laboratory's NASA Space Radiation Laboratory (NSRL), https://www.bnl.gov/nsrl/.
10. NASA Goddard Space Flight Center Radiation Effects Facility https://radhome.gsfc.nasa.gov/radhome/ref/GSFC_REF.html.
11. C. M. Castaneda, University of California at Davis (UCD) "Crocker Nuclear Laboratory (CNL) Radiation Effects Measurement and Test Facility," IEEE NSREC01 Data Workshop, pp. 77-81, Jul. 2001.
12. Edward J. Wyrwas, "AMD Radeon e9173 Low Power PCIE GPU Single Event Effects Test Report" NASA GSFC, Aug. 2022 [Online] Available: https://nepp.nasa.gov/docs/tasks/065-GPU-Devices/2022-Wyrwas-NASA-TM-19-022-AMD-e9173-2022Aug24-SEE-Test-Report-20230009291.pdf.
13. M. C. Casey, J. S. Goodwill, E. J. Wyrwas, R. A. Austin, C. M. Wilson, S. D. Stansberry, N. Gorius, and S. Aslam, "Single-Event Effects on Commercial-Off-the Shelf Edge-Processing Artificial Intelligence ASICs," in IEEE Trans. on Nucl. Sci., doi: 10.1109/TNS.2023.3286728.
14. Edward J. Wyrwas, "Proton Testing of AMD v1202b System on Chip," NASA GSFC, May 2022 [Online] Available: https://nepp.nasa.gov/docs/tasks/065-GPU-Devices/2022-Wyrwas-NASA-TM-20-005-AMD-v1202b-SoC-Proton-Test-Report-20230000488.pdf.
15. Melanie D. Berg, "Update on NEPP SEE FPGA Test and Analysis Featuring: The Lattice Avant TSMC 16 nm FinFet, The Xilinx TSMC 7nm Versal AIE Core, and Fluence to Failure Applied Methodologies" 2023 NEPP ETW, NASA GSFC, June 2022 [Online] Available: https://nepp.nasa.gov/workshops/etw2023/talks/14-JUN-WED/1000_Berg_v3_20230009399.pdf.
16. Edward P. Wilcox, "Single-Event Effect Test Report Micron MT29F16G08ABABA NAND Flash Memory," NASA GSFC, Apr. 2022 [Online] Available: 20230009623-Wilcox-NASA-TM-22-009-MT29F16G08ABABA-2022Feb-2022Apr-SEE-Test-Report.
17. Ted Wilcox & Rebekah Austin, "Applied SEE Test Data: Modern NAND Flash," SEE-MAPLD, May 2023 [Online] Available: https://www.seemapld.org/ archive.php
18. Edward P. Wilcox, "Single-Event Effects Test Report SKHynix H25G9TC18CX488 512Gb 3D NAND Flash," NASA GSFC, Nov. 2022 [Online] Available: https://nepp.nasa.gov/docs/tasks/070-Test-Reports/2022-Wilcox-NASA-TM-22-044-H25G9TC18CX488-2022Nov-SEE-Test-Report-20230009632.pdf
19. Edward P. Wilcox, Matthew B. Joplin, Melanie D. Berg, "Single-Event Effects Response of 96- and 176-Layer 3D NAND Flash Memories," to be published in the Radiation Effects Data Workshop proceedings, July 2023.
20. Edward P. Wilcox, "Proton Test Report Micron MT29F8T08EWLGEM5, MT29F8T08EWLKEM5, and SKHynix H25G9TC18CX488 NAND Flash Memories," NASA GSFC, Dec. 2022 [Online] Available: https://nepp.nasa.gov/docs/tasks/070-Test-Reports/2022-Wilcox-NASA-TM-22-042_22-043_22-044-2022Dec-Proton-Test-Report-20230009643.pdf
21. Edward P. Wilcox, "Single-Event Effects Test Report Micron MT29F8T08EWLGEM5 8Tb 3D NAND Flash," NASA GSFC, Aug. and Nov. 2022 [Online] Available: https://nepp.nasa.gov/docs/tasks/070-Test-Reports/2022-Wilcox-NASA-TM-22-042-2022Aug-2022Dec-SEE-Test-Report-20230009630.pdf
22. Edward P. Wilcox, "Single-Event Effects Test Report Micron MT29F8T08EWLKEM5 8Tb 3D NAND Flash," NASA GSFC, Nov. 2022 [Online] Available: https://nepp.nasa.gov/docs/tasks/070-Test-Reports/2022-Wilcox-NASA-TM-22-043-MT29F8T08EWLKEM5-2022Nov-SEE-Test-Report-20230009646.pdf

23. Melanie Berg, Scott Linton, John Wiemeyer, Bob Lazaravich, Megan Casey, and Hak Kim, “Mercury DDR4 Memory (4N1G72T-24BM) Proton Single Event Effects (SEE) Test Report,” Space R3 LLC, March 2023 [Online] Available: 2022-Berg-NASA-TM-4N1G72T-24BM-DDR4-2022Dec-SEE-Test-Report-20230009531.pdf
24. Jean-Marie Lauenstein, Jason M. Osheroff "Single-Event Effect Testing of the Microchip MRH25N12U3 (JANSR2N7593) n-Type Power MOSFET," NASA GSFC, Mar. 2022 [Online] Available: https://nepp.nasa.gov/docs/tasks/044a-Power-MOSFETs/2022-Lauenstein-Osheroff-NASA-TM-21-020-JANSR2N7593-20230001108.pdf.
25. Jason M. Osheroff, “Single-Event Effect Radiation Test Report of the Infineon IRF5NJ9540 p-Type Power MOSFET,” NASA GSFC, Sept. 2022 [Online] Available: https://radhome.gsfc.nasa.gov/radhome/papers/2022-Osheroff-NASA-TM-22-016-IRF5NJ9540-20220017278.pdf.
26. Kaitlyn L. Ryder, Michael J. Campola, Kevin Lynaugh, Gianfranco Barnaba, Serhat Altunc, “Single-Event Effects Test Report Microchip, TC1016 Low Dropout Voltage Regulator,” NASA GSFC, June 2022 [Online] Available: https://radhome.gsfc.nasa.gov/radhome/papers/ 2022-Ryder-Kaitlyn-NASA-TM-TC1016-SEE-Test-Report-2022Jun-20230009536.pdf.
27. Landen D. Ryder and Edward J. Wyrwas, “SSD1351 OLED Display Driver Single Event Effects Test Report,” NASA GSFC, July 2023 [Online] Available https://radhome.gsfc.nasa.gov/radhome/papers/2022-Ryder-Landen-NASA-TM-22-045-SSD1351-2022Aug-SEE-Test-Report-20230009396.pdf.
28. Matthew B. Joplin, James D. Forney "Single-Event Effect Testing of the Analog Devices AD8041ARZ Operational Amplifier," NASA GSFC, Nov. 2022 [Online] Available: https://radhome.gsfc.nasa.gov/radhome/papers/2022-Joplin-NASA-TM-22-040-AD8041ARZ-2022Nov10-SEE-Test-Report-20230000796.pdf.
29. Kaitlyn Ryder, Michael Campola, Kevin Lynaugh, Gianfranco Barnaba, Serhat Altunc, “Single-Event Effects Test Report Linear Technology, LTC3769HUF#PBF Boost Converter Controller,” NASA GSFC, June 2022 [Online] Available: https://radhome.gsfc.nasa.gov/radhome/papers/2022-Ryder-Kaitlyn-NASA-TM-LTC3769-2022June-SEE-Test-Report-20230009761.pdf.
30. Kaitlyn Ryder, Jonathan Barth, Michael Campola, Tom Carstens, Richard Hare, “Single-Event Effects Test Report Texas Instruments, OPA691 Current Feedback Operational Amplifier,” NASA GSFC, Nov. 2022 [Online] Available: https://radhome.gsfc.nasa.gov/radhome/papers/2022-Ryder-Kaitlyn-NASA-TM-OPA691-2022Nov-SEE-Test-Report-20230009762.pdf.
31. Kaitlyn L. Ryder, Jonathan D. Barth, Michael J. Campola, Matthew B. Joplin, Thomas A. Carstens, Richard Hare, “Single-Event Effects Test Report Texas Instruments, OPA842 Low-Noise Operational Amplifier,” NASA GSFC, Nov. 2022 [Online] Available: https://radhome.gsfc.nasa.gov/radhome/papers/2022-Ryder-Kaitlyn-NASA-TM-OPA842-2022Nov-SEE-Test-Report-20230009770.pdf.
32. Kaitlyn L. Ryder, Jonathan D. Barth, Michael J. Campola, Thomas A. Carstens, Richard Hare, “Single-Event Effects Test Report Texas Instruments, OPA847 Ultra-Low Noise Operational Amplifier,” NASA GSFC, Nov. 2022 [Online] Available: https://radhome.gsfc.nasa.gov/radhome/papers/2022-Ryder-Kaitlyn-NASA-TM-OPA847-2022Nov-SEE-Test-Report-20230009771.pdf.
33. Kaitlyn L. Ryder, Jonathan D. Barth, Michael J. Campola, Matthew B. Joplin, Thomas A. Carstens, Richard Hare, “Single-Event Effects Test Report Texas Instruments, OPA855 Low-Noise Operational Amplifier,” NASA GSFC, Nov. 2022 [Online] Available: https://radhome.gsfc.nasa.gov/radhome/papers/2022-Ryder-Kaitlyn-NASA-TM-OPA855-2022Nov-SEE-Test-Report-20230009783.pdf.
34. Kaitlyn L. Ryder, Jonathan D. Barth, Michael J. Campola, Matthew B. Joplin, Thomas A. Carstens, Richard Hare, “Single-Event Effects Test Report Texas Instruments, OPA856 Low-Noise Operational Amplifier,” NASA GSFC, Nov. 2022 [Online] Available: https://radhome.gsfc.nasa.gov/radhome/papers/2022-Ryder-Kaitlyn-NASA-TM-OPA856-2022Nov-SEE-Test-Report-20230009784.pdf.
35. Thomas A. Carstens, Michael J. Campola, Matthew B. Joplin, Hak S. Kim, Anthony M. Phan, “Qorvo's NBB-400 Cascadable Broadband GaAs MMIC Amplifier Single Event Effects Test Report,” NASA GSFC, Apr. 2022 [Online] Available: https://radhome.gsfc.nasa.gov/radhome/papers/2022-Carstens-NASA-TM-21-036-NBB400-2022Apr06-20230001171.pdf.
36. Kaitlyn Ryder, Michael Campola, Kevin Lynaugh, Gianfranco Barnaba, Serhat Altunc, “Single-Event Effects Test Report Guerrilla RF, GRF 2073 Ultra-Low Noise Amplifier (LNA),” NASA GSFC, July 2022 [Online] Available: https://radhome.gsfc.nasa.gov/radhome/papers/2022-Ryder-Kaitlyn-NASA-TM-GRF2073-2022June-SEE-Test-Report-20230009787.pdf.
37. Kaitlyn Ryder, Michael Campola, Kevin Lynaugh, Gianfranco Barnaba, Serhat Altunc, “Single-Event Effects Test Report Guerrilla RF, GRF 5110 Power Low Noise Amplifier (LNA),” NASA GSFC, June 2022 [Online] Available: https://radhome.gsfc.nasa.gov/radhome/papers/2022-Ryder-Kaitlyn-NASA-TM-GRF5110-2022June-SEE-Test-Report-20230009789.pdf.
38. Megan Casey and Jonathan Barth, “Dragonfly Mass Spectrometer (DraMS) Micro-Electromechanical System (MEMS) Pirani Sensor Single-Event Effects Characterization Report,” NASA GSFC, July 2022 [Online] Available: https://radhome.gsfc.nasa.gov/radhome/papers/2022-Casey-NASA-TM-22-011-HVS-VAC03k_HVS-VAC04-2022July-SEE-Test-Report-20230009790.pdf.
39. Kaitlyn Ryder, Michael Campola, Kevin Lynaugh, Gianfranco Barnaba, Serhat Altunc, “Single-Event Effects Test Report Texas Instruments, LMX24485ESQ/NOPM Phase Locked Loop (PLL),” NASA GSFC, June 2022 [Online] Available: https://radhome.gsfc.nasa.gov/radhome/papers/2022-Ryder-Kaitlyn-NASA-TM-LMX24485ESQ-NOPM-2022June-SEE-Test-Report-20230009792.pdf.
40. Thomas A. Carstens, Anthony M. Phan, Michael J. Campola, Matthew B. Joplin, “Texas Instrument DRV8881 2.5A Dual H-Bridge Motor Driver Heavy-Ion Single-Event Effects Test Report,” NASA GSFC, Nov. 2022 [Online] Available: https://radhome.gsfc.nasa.gov/radhome/papers/2022-Carstens-NASA-TM-22-014-DRV8881-2022Nov11-SEE-Test-Report-20230008542.pdf.

41. Thomas A. Carstens, Michael J. Campola, Anthony M. Phan, Hak S. Kim, “MAX1340 12-Bit, Multichannel ADCs/DACs Single-Event Effects Characterization Test Report Using Heavy Ions,” NASA GSFC, Nov. 2022 [Online] Available: https://radhome.gsfc.nasa.gov/radhome/papers/2022-Carstens-NASA-TM-22-015-MAX1340-2022Nov11-SEE-Test-Report-20230001253.pdf.
42. Thomas A. Carstens, Anthony M. Phan, Michael J. Campola, “Infineon’s TLE4309 Adjustable Linear Low Dropout LED Driver Single-Event Effects Characterization Test Report Using Heavy Ions,” NASA GSFC, Nov. 2022 [Online] Available: https://radhome.gsfc.nasa.gov/radhome/papers/2022-Carstens-NASA-TM-22-013-TLE4309-2022Nov09-SEE-Test-Report-20230001865.pdf.
43. Michael J. Campola, Anthony M. Phan, Landen Ryder, Christina Seidleck, Tom Carstens, “Single-Event Effect Testing of the Broadcom ACPL-785E Optocoupler,” NASA GSFC, Dec 2020 [Online] Available: https://radhome.gsfc.nasa.gov/radhome/papers/2020-Campola-Phan-Landen-Ryder-TR-17-047-ACPL-785E-Optocoupler-2020Dec19-NASA-TM-20210025964.pdf.
44. Michael J. Campola, Anthony M. Phan, Landen Ryder, Christina Seidleck, Tom Carstens, “Single-Event Effect Testing of the Broadcom ACPL-785E Optocoupler,” NASA GSFC, Mar. 2022 [Online] Available: https://radhome.gsfc.nasa.gov/radhome/papers/(2022-Campola-Phan-Landen-Ryder-TR-17-047-ACPL-785E-Optocoupler-2022Mar-NASA-TM-20230009843.pdf.
45. Melanie D. Berg, Hak S. Kim, Anthony M. Phan, Michael J. Campola, Jim Tavacoli, “Lattice Semiconductor CrossLink-NX FPGA LIFCL-40-9BG400C Total Ionizing Dose Test Report,” NASA GSFC, Mar. 2021 and Sept. 2022 [Online] Available: https://nepp.nasa.gov/docs/tasks/054-FPGA-Radiation-Testing/2022-Berg-NASA-TM-21-016-LIFCL-40-9BG400C-2021Mar-2022Aug-TID-Test-Report-20230000917.pdf
46. Thomas A. Carstens, Hak S. Kim, Michael J. Campola, Edward P. Wilcox, "PE99155 Point-Of-Load Buck Regulator Total Ionizing Dose Test Report," NASA GSFC, Feb. 2022 [Online] Available: https://radhome.gsfc.nasa.gov/radhome/papers/2022-Carstens-NASA-TM-19-001-Teledyne-e2v-PE99155-2022Feb10-TID-Test-Report-20230004065.pdf.
47. Edward P. Wilcox, Jean-Marie Lauenstein, “Proton Test Report Micropac 53253-119 Dual Power MOSFET Optocoupler,” May. 2022 [Online] Available: https://radhome.gsfc.nasa.gov/radhome/papers/2022-Wilcox-TM-22-039-Micropac-53253-119-2022May17-Proton-Test-Report-20230009836.pdf.
48. Edward P. Wilcox, Jean-Marie Lauenstein, “Proton Test Report Micropac 53111 Power MOSFET Optocoupler,” May. 2022 [Online] Available: https://radhome.gsfc.nasa.gov/radhome/papers/2022-Wilcox-TM-21-030-Micropac-53111-2022May17-Proton-Test-Report-20230009837.pdf.
49. Edward P. Wilcox, Jean-Marie Lauenstein, Alyson D. Topper, “Proton Test Report Micropac 66212-300 Optocoupler,” NASA GSFC, May 2022 [Online] Available: https://radhome.gsfc.nasa.gov/radhome/papers/2022-Wilcox-TM-19-047-66212-2021Oct07-2022May-Proton-Test-Report-20220010398.pdf.
50. Landen D. Ryder, Edward J. Wyrwas, and Geraldo A. Cisernos, “Commercial-Off-The-Shelf Small-Form Factor Organic LED and Liquid Crystal Displays Displacement Damage and Total Ionizing Dose Test Report,” NASA GSFC, Sept. 2022 [Online] Available: https://radhome.gsfc.nasa.gov/radhome/papers/2022-Ryder-Landen-NASA-TM-22-045_22-046_22-048_22-051-2022Sept28-DD-TID-Test-Report-20230009397.pdf.
51. Landen D. Ryder, Edward J. Wyrwas, Geraldo A. Cisneros, Justin R. Bautista, Xiaojing Xu, Tyler M. Garrett, Michael J. Campola, Razvan Gaza, “An Examination of the Radiation Sensitivity of Electronic Display Pixel Technologies,” to be published in the Radiation Effects Data Workshop proceedings, July 2023.
52. Megan Casey and Rebekah Austin, “MEMS Pirani Displacement Damage Dose Characterization Test Report,” NASA GSFC, July 2022 [Online] Available: https://radhome.gsfc.nasa.gov/radhome/papers/2022-Casey-NASA-TM-22-011-HVS-VAC03k_HVS-VAC04-Pirani-MEMS-2022July-DD-Test-Report-20230009838.pdf.
53. Aubin P. Antonsanti, Alexandre Le Roch, Landen Ryder, and Jean-Marie Lauenstein, "Sony IMX219PQ Image Sensor Total Ionizing Dose Test Report," NASA GSFC, Nov. 2022 [Online] Available: https://nepp.nasa.gov/docs/tasks/044a-Power-MOSFETs/2022-Antonsanti-Lauenstein-NASA-TM-22-052-IMX219PQ-2022Nov-20230009984.pdf.
54. Landen Ryder, Jean-Marie Lauenstein, Marc Matyseck, “C30665L CD3740 Displacement Damage and Total Ionizing Dose Test Report,” NASA GSFC, May 2022 [Online] Available: https://radhome.gsfc.nasa.gov/radhome/papers/2022-Ryder-Landen-NASA-TM-21-029-C30665L-CD3740-2022May-20230008953.pdf.